IMUAngle: Joint Angle Estimation with Inertial Sensors in Daily Activities

Lena Uhlenberg
Chair of Digital Health
FAU Erlangen-Nürnberg, Germany
lena.uhlenberg@web.de

Swathi Hassan Gangaraju
Chair of Digital Health
FAU Erlangen-Nürnberg, Germany
swathihg2009@gmail.com

Oliver Amft
University of Freiburg, Germany
Hahn-Schickard, Germany
FAU Erlangen-Nürnberg, Germany
amft@computer.org

ABSTRACT

We present a framework for IMU-based joint angle estimation during activities of daily living (ADL). Personalised musculoskeletal models were created from anthropometric data. Three sensor fusion algorithms were optimised to estimate orientation from IMU data and used as input for the simulation framework. Four ADLs, involving upper and lower limbs were simulated. Joint kinematics of IMU-based simulations were compared to optical marker-based simulations. Results for IMU-based simulations showed median RMSE of $0.8 - 15.5\,^{\circ}$ for lower limbs and $1.5 - 33.9\,^{\circ}$ for upper limbs. Median RMSE were $4.4\,^{\circ}$, $5.8\,^{\circ}$, $6.9\,^{\circ}$, $6.5\,^{\circ}$ for ankle plantarflexion, knee-, hip flexion, and hip rotation, respectively. For upper limbs, elbow flexion showed best median RMSE $\sim 3.7\,^{\circ}$, whereas elevation angles ($\sim 24.5\,^{\circ}$) and shoulder rotation ($\sim 12.5\,^{\circ}$) performed worst. Increased RMSE at upper limbs was attributed to the degrees of freedom at the shoulder region compared to the hip. Overall, transversal plane movements (rotations) showed higher median RMSE compared to sagittal plane movements (flexion/extension). Optimisation of orientation estimators improved performance considerably depending on ADL (up to $\sim 20\,^{\circ}$). Comparing sensor fusion algorithms, Madgwick and Mahony produced comparable joint kinematics, whereas the Extended Kalman Filter performance showed larger variability depending on the ADL. Our approach offers a realistic representation of joint kinematics and can be supported by optimising parameters of sensor fusion algorithms.

CCS CONCEPTS

• **Human-centered computing → Ubiquitous and mobile computing design and evaluation methods**.

KEYWORDS

Wearable inertial sensors, joint kinematics, multiscale modelling

ACM Reference Format:
Lena Uhlenberg, Swathi Hassan Gangaraju, and Oliver Amft. 2022. IMUAngle: Joint Angle Estimation with Inertial Sensors in Daily Activities. In *The 2022 International Symposium on Wearable Computers (ISWC '22), September 11–15, 2022, Cambridge, United Kingdom.* ACM, New York, NY, USA, 5 pages. https://doi.org/10.1145/3544794.3558470

ISWC '22, September 11–15, 2022, Cambridge, United Kingdom

ACM ISBN 978-1-4503-9424-6/22/09.
https://doi.org/10.1145/3544794.3558470

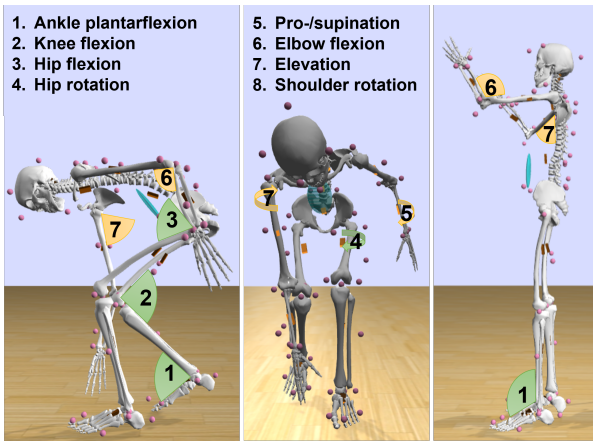

Figure 1: Illustration of joint angles considered for all ADLs.

1 INTRODUCTION

Wearable inertial measurement units (IMUs) are used to quantify motion performance, including execution quality and skill assessments, e.g. in daily living, sports, and rehabilitation [3, 11]. While relative orientation of limb segments, i.e. joint angles, are often considered to be key indicators of motion performance (incorrect loading, disease patterns, etc.), their estimation with IMUs is known to be challenging. IMU manufacturers offer proprietary solutions that are not reproducible using open-source algorithms and cannot be implemented with alternative IMUs. Furthermore, common activities of daily living (ADLs) have been given insufficient consideration in IMU-MoCap analyses. Recently, the new OpenSense workflow has been integrated into the well-established open-source musculoskeletal modelling software OpenSim to support biomechanical simulations based on IMU data [2].

In this work, we investigate an IMU-based simulation of activities of daily living (ADLs) to establish a performance baseline for estimating joint angles using an open-source framework. In particular, this paper provides the following contributions:

(1) We present a framework to derive full-body 3D joint kinematics with body-worn IMU sensors and using personalised biomechanical models.
(2) We evaluate IMU-based estimation performance of eight joint angles against optical motion-capture (MoCap) in four ADLs. IMU data and the gold-standard MoCap data were simultaneously captured in ten participants.
(3) We compare joint angle estimation across sensor fusion algorithms after optimising their parameters using leave-one-participant-out cross-validation. Orientation estimates served as input to the biomechanical ADL simulations.

We believe that the pipeline proposed in this work and our performance analyses can assist wearable system researchers and designers to determine realistic error ranges for joint angle estimation with IMUs depending on expected activities.

2 RELATED WORK

Previous studies have estimated lower limb kinematics using IMUs with joint angle root-mean-square-error (RMSE) of $5 - 10\,^{\circ}$, compared to MoCap-based kinematics and found larger agreement of angles in the sagittal plane compared to the other two planes [8, 12]. So far, OpenSense has been used exclusively to simulate lower limbs during walking, in particular to analyse kinematic drift in 10-min walking trials and motion variability in gait [1, 2]. In contrast, upper limb kinematics in daily activities have not been sufficiently addressed by IMU-based analyses. Goodwin et al. [4] monitored the humeral elevation in patients with spinal cord injuries and concluded that IMU-based methods for quantifying shoulder movement show good agreement with MoCap. Picerno et al. [7] developed a calibration procedure using anatomical landmarks for shoulder/elbow kinematics. However, only uni-axial movements were measured.

Few IMU-based studies showed accuracy measures (e.g. waveform similarities, amplitude) corresponding with upper limb joint kinematics estimates. Wang et al. [13] compared joint angles from five IMUs mounted at one upper body side, a markerless MoCap system, and standard marker-based method. They found smaller joint angle RMSE at shoulders than elbows. Moreover, closed-source systems and algorithms (e.g. Xsens sensors with proprietary algorithms) had been used for joint angle estimation, which may be expensive or limited to specific settings, hardware, etc. [2]. In this work, we analyse several ADLs and joint angles, involving both, upper and lower limbs, to explore estimation errors and demonstrate versatility of IMU-based kinematic simulations.

3 METHODS

Figure 2: Method overview. IMU and MoCap data were processed to create personalised biomechanical models. Orientation estimates based on IMU data and sensor fusion algorithms were used in OpenSense to animate biomechanical models in ADL simulations. After parameter optimisation, IMU-based joint angle estimates were compared to MoCap.

3.1 Personalised biomechanical body models

We used the OpenSim full-body thoracolumbar spine model [10], which, in contrast to previous IMU-based simulations [1, 2], accounts for the degrees of freedom (DOF) at upper limbs and spine areas. Body models were personalised using OpenSim, including scaling (changing body mass properties and dimensions according to distances between model landmarks) and registering markers attached to study participants. Thus, modelling input included body weight and MoCap marker data.

3.2 Sensor fusion algorithms

Three sensor fusion algorithms were tested to estimate orientation in quaternions q based on Python AHRS (https://ahrs.readthedocs.io): (1) Madgwick filter [5] is a gradient-descent algorithm with filter gain β representing mean zero gyroscope measurement errors, expressed as $\beta = \sqrt{\frac{3}{4}}\bar{\omega}_\beta$, where $\bar{\omega}_\beta$ is the estimated mean zero gyroscope measurement error of each axis. (2) Mahony filter [6] is a deterministic kinematic observer driven by attitude and angular velocity measurements and tuned by proportional gain K_p and integral gain K_i. (3) Extended Kalman Filter (EKF) [9] is a nonlinear Kalman filter, with measurement noise variance (N_v) as main parameter. Local tangent plane coordinate frame was set to geographical East, North, and Up directions (x,y,z), local magnetic field was set to Munich, Germany.

3.3 OpenSense

The automated OpenSense workflow consists of five steps to prepare for ADL simulation: (1) Preprocessed MoCap and IMU quaternions were imported and assigned to the body models. (2) A custom sensor mapping was applied for IMUs to link with corresponding rigid body parts (pelvis, thigh, etc.), represented as a "Frame" (orthogonal XYZ coordinate system). (3) Initial IMU orientations were defined relative to body segments according to a static reference trial. (4) MoCap and static IMU reference data were used to determine IMU orientations relative to body model segments as fixed rotational offsets. (5) Rotation offsets were assigned to IMU "Frames", yielding calibrated body models.

3.4 ADL simulation

Estimated quaternions per fusion algorithm and ADL data were used as input into the OpenSense inverse kinematic solver to estimate joint angles by minimising weighted squared differences. We reduced relative weighting of distal IMUs (tibial and foot) to minimise influence of in-ground metal force plates [2]. Four ADLs involving upper and lower limb movements were analysed: shelve ordering (SO), stairs climbing (SC), walking (W), and pen pickup (PP). ADLs were selected to cover a variety of daily body movements and involve multiple limbs.

3.5 Evaluation study

We included ten healthy volunteers. Participants gave written consent and ethics approval was granted by an institutional ethics committee. We derived body segment masses and joint centres using Visual3D (C-Motion Inc., USA). See Tab. 1 for details.

Table 1: Study participant data. F: Female. M: Male.

ID	Height [m]	Weight [kg]	Age [years]	Sex [F/M]	ID	Height [m]	Weight [kg]	Age [years]	Sex [F/M]
P1	1.80	74	25	M	**P6**	1.69	62	24	F
P2	1.71	56	23	F	**P7**	1.70	65	29	M
P3	1.78	65	29	M	**P8**	1.65	62	28	F
P4	1.83	79	25	M	**P9**	1.73	66	22	F
P5	1.68	68	36	F	**P10**	1.45	48	21	F

A total of 54 reflective spherical MoCap markers were placed at anatomical landmarks and 16 IMUs (MyoMotion, Noraxon, USA) were attached to each body segment. To ensure tight fixation of IMUs, Noraxon velcro straps with IMU pockets were used (see Fig. 6A). A synchronized and calibrated 11-camera marker-based MoCap system (Qualisys, Sweden) was used to acquire gold-standard MoCap data. Cameras and IMUs were time-synchronized at a frame rate of 100 Hz. MoCap data was filtered by a 6 Hz lowpass Butterworth filter. A static reference trial was performed to reconstruct

body segments, determine dimensions, joint centres, segment coordinate systems, and calibrate IMU sensors. Subsequently, participants were asked to perform each ADL three times. Labelling and MoCap marker gap filling was performed with Qualysis Track Manager, v. 2018. Recording time was ~30 min±10 min per participant. We have considered eight joint angles at upper and lower limbs to cover the full body, as shown in Fig. 1. However, only two IMUs are needed to estimate one segment angle, with IMUs located below and above the respective joint.

3.6 Optimisation and error analysis

Leave-One-Participant-Out cross-validation (LOPOCV) was used to fit parameters of sensor fusion algorithms (β; {K_p,K_i}; N_v) per ADL. Participant data that was held-out during training was used for error analysis and results averaged over all folds.

Joint angle estimation performance was evaluated by deriving RMSE between IMU-based simulations and MoCap measurements for each participant and ADL. As some data were not normally distributed, median and interquartile range (IQR) were computed over all participants. Outliers were defined as > 1.5×IQR below or above the 25th and 75th percentile.

4 RESULTS

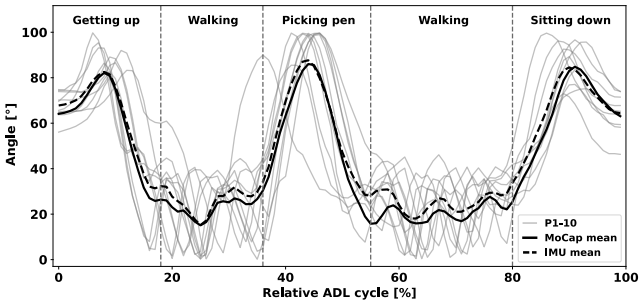

Figure 3: Illustration of hip flexion angle estimates (Madgwick, $\beta = 0$) for ADL 'Pen pickup' of all participants (P1-10).

Fig. 3 shows time series overlay of hip flexion for ADL 'Pen pickup' for all participants using Madgwick filter ($\beta = 0$). One ADL cycle is divided into five consecutive movements starting from upright sitting (0%): (1) Getting up from the chair by leaning forward with the upper body, thus increasing hip flexion, followed by full hip extension when standing (~18%). (2) Walking forward, i.e. a cyclic variation in hip flexion per stride (~36%). (3) Pen pickup motion, thus increase in hip flexion to reach downwards (~55%). (4) Walking back (~80%), and (5) sitting down on the chair, thus a peak and subsequent decrease in hip flexion towards sitting upright (100%). Natural deviations between participants, e.g. while walking, were caused by different walking speeds and stride lengths.

Fig. 4 shows a parameter sweep for sensor fusion algorithms to optimise mean RMSE across all joint angles for for the ADL SO. Increasing $\beta > 0.1$ for the Madgwick filter reduced performance for all ADLs. While for SO, the optimum was $\beta = 0.1$, further analyses of other ADLs yielded best performance for $\beta = 0$. For Mahony filter, $K_i = 0$ and $K_p = 0.1$ gave the best performance for SO and SC. For W and PP, $K_i = 0$ and $K_p = 0.0$ were better. Optimising N_v of the EKF resulted in $N_v = 0.0, 0.0, 0.01$ for SO, $N_v = 0.0, 0.0, 0.17$ for SC and PP, and $N_v = 0.01, 0.06, 0.41$ for W. EKF parameters showed

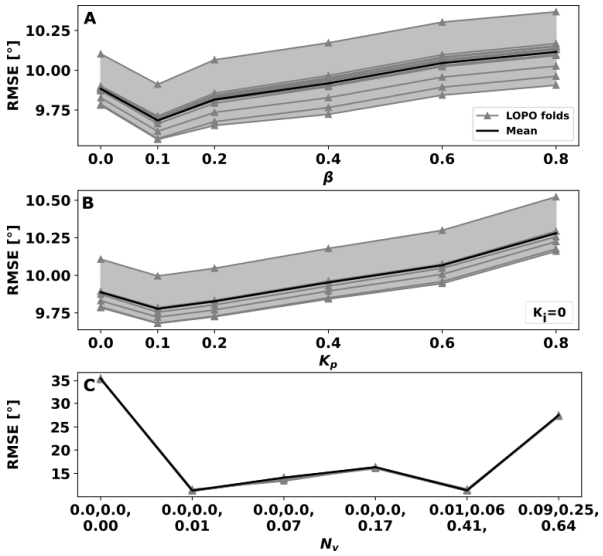

Figure 4: Parameter sweep for sensor fusion algorithms to optimise mean RMSE across all joint angles of the ADL 'Shelve ordering'. A: Madgwick filter. B: Mahony filter. C: EKF.

the largest variation across ADLs, with differences of up to 20 ° for the considered joint angles (see Fig. 4C).

As the evaluation of joint kinematics is one of the main research components in the investigation of motion performance Fig. 5 shows RMSE averaged over participants per filter design and ADL. Overall, lower limbs (Fig. 5A) showed lower RMSE compared to upper limbs (Fig. 5B). SO had minimal errors at lower limbs, which can be attributed to the lack of movement during the ADL. Overall, joint angle errors were 4.4 °, 5.8 °, 6.9 °, 6.5 ° for ankle plantarflexion, knee-, hip flexion and hip rotation, respectively. Among sensor fusions algorithms, Madgwick and Mahony filters produced similar kinematics per joint angle. Depending on joint angle and ADL, EKF performed similar or inferior to the two other filters, with RMSE between ~1 − 11 ° at lower limbs.

At upper limbs, elbow flexion showed lowest error (~3.7 °), whereas pro-/supination (~5.1 °) and arm elevation angles had largest errors (~24.5 °), in particular for SO. Hand pro-/supination are key movements of SO, with largest median RMSE compared to other ADLs. Overall arm elevation showed highest RMSE for all filters and ADLs, except W; followed by shoulder rotation (~12.5 °). Among sensor fusions algorithms, only minor error differences were observed at upper limbs, favouring the Madgwick algorithm.

Fig. 6B and C illustrates errors incurred by the IMU-based simulation approach compared to MoCap. For SO trials, we observed lower arm elevation and shoulder rotation, resulting in reduced overall arm height and a larger wrist to wrist distance (Fig. 6B). For PP, IMU-based simulations resulted in smaller hip flexion angles at lower limbs, resulting in increased wrist to floor distance (Fig. 6C).

5 DISCUSSION

Overall median RMSE was 5.6 ° for lower limbs, with median RMSE range between 0.8 − 12.0 °, except for hip rotation. Joint angle estimation performances for lower limbs are in agreement with literature. For example, Al Borno et al. [2] reported median RMSE between 3 − 6 ° for lower limb joint angles, except hip rotation (12 °),

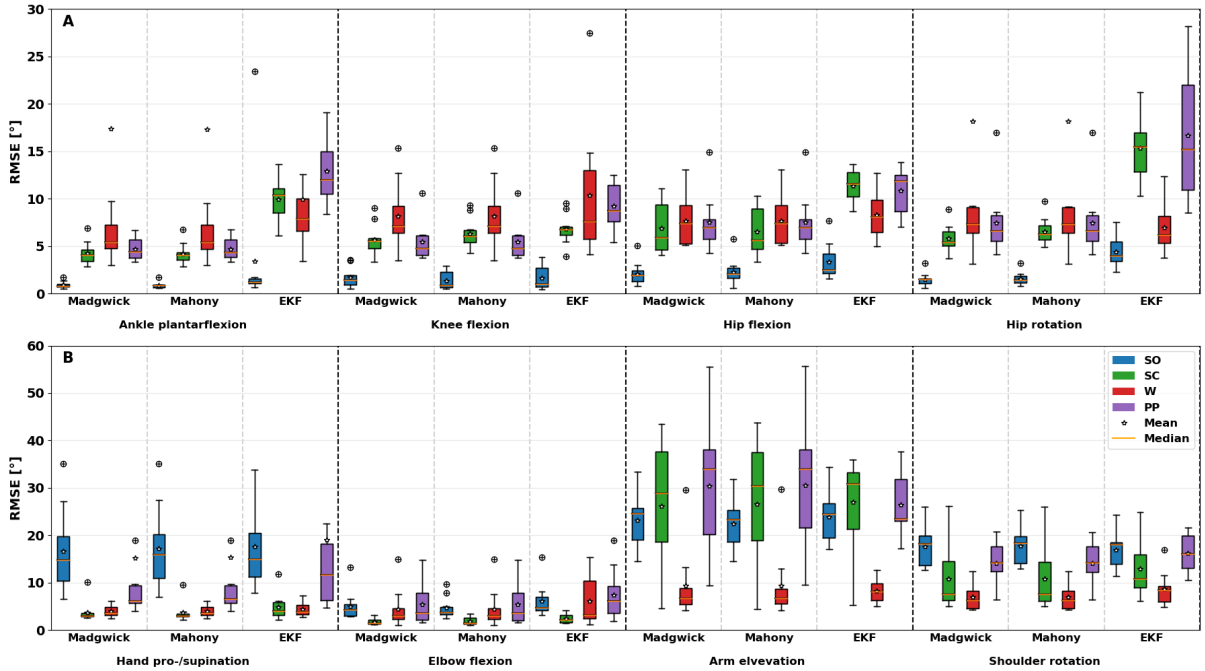

Figure 5: A: RMSE per ADL of lower limbs. B: RMSE per ADL of upper limbs. ADLs were: shelve ordering (SO), stairs climbing (SC), walking (W), and pen pickup (PP).

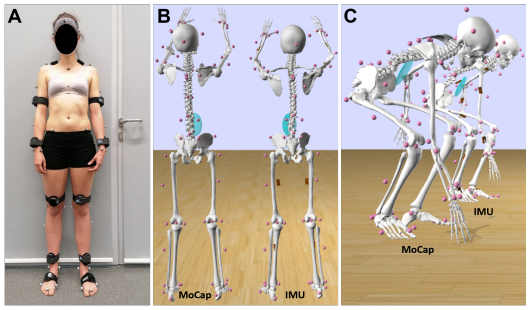

Figure 6: Study setup and examples of IMU-based simulation issues. A: Study participant with Noraxon IMUs and MoCap markers. B: Less shoulder rotation and elbow flexion during SO. C: Less hip flexion and a more upright upper body position during PP, thus not reaching the floor.

during 10-min walk trials using Madgwick and Mahony filters. Furthermore, Bailey et al. [1] reported stride-to-stride variability during treadmill gait of 4.4 – 6.7 ° for knee, ankle, and hip flexion, as well as hip rotation using the Madgwick filter.

For upper limbs, our median RMSE ranged between 1.5 – 33.9 °, with arm elevation angles showing largest errors. Overall median RMSE was below 10 °. In comparison, Wang et al. [13] reported median RMSE for their 5-IMU system ranging between 23.8 – 62.6 °, with overall median RMSE below 30 ° across activities. IMUs were mounted at one side of the upper body and tended to overestimate shoulder rotation. Picerno et al. [7] estimated uni-axial arm elevation in frontal, scapular, and sagittal planes with 3° and elbow flexion-extension with an error of 2 ° compared to an optoelectronic stereophotogrammetric system. Our results showed larger median RMSE for elbow flexion (3.4 °) and shoulder rotation (12.5 °), which could be explained by multi-axial ADL motions. So far, related work considered either upper or lower limbs, whereas ADLs are usually a combination of both. Furthermore, leave-one-participant-out cross-validation was not reported as an evaluation strategy. Compared to some proprietary IMU solutions (e.g. Noraxon Ultimum Motion), our study found larger errors. However, in contrast to proprietary systems, our approach could be implemented with different IMUs.

6 CONCLUSION

We modelled full-body 3D joint kinematics with body-worn IMU sensors using personalised biomechanical models. Our IMU-based framework can estimate joint angles in dynamic motion simulations of typical ADLs and can be used to optimise parameters of frequently used sensor fusion algorithms. The IMU-based simulations produced joint kinematics that were consistent with MoCap, thus confirming their validity for kinematic analyses in wearable systems. In general, lower limbs yielded smaller RMSE than upper limbs, which could be attributed to the larger DOF at upper limbs, in particular for shoulders, and thus resulting in a more challenging modelling task. With the open-source OpenSense toolbox, our approach enhances reproducibility compared to previously published modelling and simulation techniques, in particular with regard to complex upper limb analyses. Future work may include improvements of the biomechanical body model, targeting shoulder DOF, and further optimisation of sensor fusion algorithm parameters, e.g. optimise limbs- or position-specific filters.

ACKNOWLEDGMENTS

We thank Juan Carlos Suarez Mora, as well as FAU LTD group and Med 3 of the University Medical Center Erlangen for their support in the study implementation and data preprocessing. Furthermore, we thank Al Borno et al. [2] for or sharing their data via OpenSimTK.

REFERENCES

[1] Christopher A. Bailey, Thomas K. Uchida, Julie Nantel, and Ryan B. Graham. 2021. Validity and Sensitivity of an Inertial Measurement Unit-Driven Biomechanical Model of Motor Variability for Gait. (Sept. 2021), 2021.09.27.461967.

[2] Mazen Al Borno, Johanna O'Day, Vanessa Ibarra, James Dunne, Ajay Seth, Ayman Habib, Carmichael Ong, Jennifer Hicks, Scott Uhlrich, and Scott Delp. 2021. OpenSense: An Open-Source Toolbox for Inertial-Measurement-Unit-Based Measurement of Lower Extremity Kinematics over Long Durations. *bioRxiv* (July 2021), 2021.07.01.450788. https://doi.org/10.1101/2021.07.01.450788

[3] Adrian Derungs, Sebastian Soller, Andreas Weishäupl, Judith Bleuel, Gereon Berschin, and Oliver Amft. 2018. Regression-Based, Mistake-Driven Movement Skill Estimation in Nordic Walking Using Wearable Inertial Sensors. In *Proceedings of the 2018 IEEE International Conference on Pervasive Computing and Communications (PerCom)*. Athens, 1–10. https://doi.org/10.1109/PERCOM.2018.8444576

[4] Brianna M. Goodwin, Stephen M. Cain, Meegan G. Van Straaten, Emma Fortune, Omid Jahanian, and Melissa M. B. Morrow. 2021. Humeral Elevation Workspace during Daily Life of Adults with Spinal Cord Injury Who Use a Manual Wheelchair Compared to Age and Sex Matched Able-Bodied Controls. *PLoS ONE* 16, 4 (April 2021). https://doi.org/10.1371/journal.pone.0248978

[5] Sebastian O H Madgwick, Andrew J L Harrison, and Andrew Vaidyanathan. 2011. Estimation of IMU and MARG Orientation Using a Gradient Descent Algorithm. *IEEE International Conference on Rehabilitation Robotics : [proceedings]* 2011 (2011), 5975346. https://doi.org/10.1109/icorr.2011.5975346

[6] Robert Mahony, T. Hamel, P. Morin, and Ezio Malis. 2012. Nonlinear Complementary Filters on the Special Linear Group. *International Journal of Control - INT J CONTR* 85 (Oct. 2012), 1–17. https://doi.org/10.1080/00207179.2012.693951

[7] Pietro Picerno, Pietro Caliandro, Chiara Iacovelli, Chiara Simbolotti, Michele Crabolu, Danilo Pani, Giuseppe Vannozzi, Giuseppe Reale, Paolo Maria Rossini, Luca Padua, and Andrea Cereatti. 2019. Upper Limb Joint Kinematics Using Wearable Magnetic and Inertial Measurement Units: An Anatomical Calibration Procedure Based on Bony Landmark Identification. *Scientific Reports* 9 (Oct. 2019). https://doi.org/10.1038/s41598-019-50759-z

[8] Xavier Robert-Lachaine, Hakim Mecheri, Christian Larue, and André Plamondon. 2017. Validation of Inertial Measurement Units with an Optoelectronic System for Whole-Body Motion Analysis. *Medical & Biological Engineering & Computing* 55, 4 (April 2017), 609–619. https://doi.org/10.1007/s11517-016-1537-2

[9] Angelo Maria Sabatini. 2011. Kalman-Filter-Based Orientation Determination Using Inertial/Magnetic Sensors: Observability Analysis and Performance Evaluation. *Sensors* 11, 10 (Oct. 2011), 9182–9206. https://doi.org/10.3390/s111009182

[10] Stefan Schmid, Katelyn A. Burkhart, Brett T. Allaire, Daniel Grindle, and Dennis E. Anderson. 2020. Musculoskeletal Full-Body Models Including a Detailed Thoracolumbar Spine for Children and Adolescents Aged 6 - 18 years. *3rd International Workshop on Spine Loading and Deformation* 102 (March 2020), 109305. https://doi.org/10.1016/j.jbiomech.2019.07.049

[11] Gabriele Spina, Guannan Huang, Anouk W. Vaes, Martijn A. Spruit, and Oliver Amft. 2013. COPDTrainer: A Smartphone-Based Motion Rehabilitation Training System with Real-Time Acoustic Feedback. In *Ubicomp 2013: Proceedings of the 2013 ACM International Joint Conference on Pervasive and Ubiquitous Computing*. ACM, 597–606. https://doi.org/10.1145/2493432.2493454

[12] Wolfgang Teufl, Markus Miezal, Bertram Taetz, Michael Fröhlich, and Gabriele Bleser. 2019. Validity of Inertial Sensor Based 3D Joint Kinematics of Static and Dynamic Sport and Physiotherapy Specific Movements. *PLOS ONE* 14, 2 (Feb. 2019), e0213064. https://doi.org/10.1371/journal.pone.0213064

[13] Sophie L. Wang, Gene Civillico, Wesley Niswander, and Kimberly L. Kontson. 2022. Comparison of Motion Analysis Systems in Tracking Upper Body Movement of Myoelectric Bypass Prosthesis Users. *Sensors (Basel, Switzerland)* 22, 8 (April 2022). https://doi.org/10.3390/s22082953